

Constraints on Einstein-dilation-Gauss-Bonnet gravity and electric charge of compact binary systems from GW230529

Bo Gao,^{1,2} Shao-Peng Tang,¹ Hai-Tian Wang,^{3,*} Jingzhi Yan,^{1,2,†} and Yi-Zhong Fan^{1,2}

¹Key Laboratory of Dark Matter and Space Astronomy,

Purple Mountain Observatory, Chinese Academy of Sciences, Nanjing 210033, China

²School of Astronomy and Space Science, University of Science and Technology of China, Hefei, Anhui 230026, China

³Kavli Institute for Astronomy and Astrophysics, Peking University, Beijing 100871, China

(Dated: July 15, 2024)

In this work, we study the implications of GW230529 on gravity theories and the charge of black holes. The GW230529, which was initially released in O4a, is most likely neutron star-black hole (NSBH) mergers. We reanalyze the data from the GW230529 event to obtain bounds on the Einstein-dilation-Gauss-Bonnet (EdGB) gravity parameter $\sqrt{\alpha_{\text{EdGB}}}$ and the electric charge of compact binary systems. The event places a 90% credible upper bounds on $\sqrt{\alpha_{\text{EdGB}}}$ of $\lesssim 0.298$ km. After including high order corrections of EdGB gravity, the bounds improve to $\sqrt{\alpha_{\text{EdGB}}} \lesssim 0.260$ km. Analyses of GW230529 also yield a 90% credible upper bounds on the combination of charge-to-mass ratio of the binary components $\zeta \lesssim 0.024$. The constraints are more stringent than those derived from previously observed single gravitational wave merger event.

I. INTRODUCTION

The fourth observing run (O4) of the Advanced LIGO (aLIGO), Advanced Virgo, and KAGRA observatory network (LVK) commenced on 24 May 2023. The first part of the fourth observing run (O4a) concluded at 16:00 UTC on 16 January 2024. Shortly after the start of O4a, aLIGO detected a gravitational wave (GW) signals GW230529.181500 (hereafter referred to as GW230529) with a signal-to-noise ratio (SNR) of 11.6. GW230529 was emitted from the coalescence of a compact binary star with masses in the ranges of $2.5 - 4.5 M_{\odot}$ and $1.2 - 2.0 M_{\odot}$, as measured at the 90% credible intervals [1]. The analysis of GW230529 does not provide information about the tidal deformability of the secondary object and the primary object's tidal deformability is estimated to peak at zero. Based on the GW data alone, definitively identifying the components of GW230529 is remains challenging. However, by considering existing estimations for the maximum neutron star mass [2], the most plausible interpretation is that GW230529 resulted from the merger of a neutron star and a black hole. Notably, the extended inspiral signals observed by aLIGO in GW230529 could provide more stringent constraints on deviations from general relativity or the presence of charge in black holes within the parameterized post-Einsteinian (ppE) framework [3, 4]

Scalar Gauss-Bonnet (sGB) gravity extends General Relativity (GR) by incorporating a dynamical scalar field coupled to the Gauss-Bonnet invariant. This modification introduces a coupling constant α_{GB} , which has a dimension of length squared. The literature on sGB gravity and its implications is extensive and continues to evolve (see, for instance, Refs. [5, 6] for comprehensive reviews and Refs. [7–13] for recent developments). A particular variant of sGB gravity, Einstein-dilaton Gauss-Bonnet (EdGB) gravity, introduces a dilaton scalar field, motivated by string theory and cosmolog-

ical inflationary models [14, 15]. Significant effort has been devoted to constraining the parameter $\sqrt{\alpha_{\text{EdGB}}}$, with a comprehensive summary available in Table I. In addition to studying constraints from ground-based GW detectors, there are some researches on constraints from future space-based GW detectors. For instance, the TianQin mission is expected to refine these constraints to an order of $O(0.1)$ km using extreme mass ratio GW sources [16]. Additionally, the capability of space-based GW observatories such as LISA, TianQin, and Taiji to constrain EdGB gravity has been discussed in recent literature [17–19]. For events involving high-mass systems, the quasinormal mode corrections of EdGB gravity are significant [20]. GW from extreme mass ratio inspirals have also gained noticeable attention due to their potentiality in testing deviations from Kerr geometry [21, 22]. This paper focuses on the corrections in the inspiral phase, as both components of GW230529 are of relatively low mass.

Astrophysical black holes (BHs) are typically assumed to be Kerr black holes due to de-charging processes from their surrounding environments. However, GR [33, 34] and theories beyond the Standard Model [35] suggest that BHs can possess various types of charges. Moreover, observational evidence confirming the charge neutrality of BHs remains elusive. Consequently, there is a strong impetus to determine the electric charge of BHs. Several methodologies have been developed to limit the electric charge of BHs. For example, imaging supermassive black holes with the Event Horizon Telescope has provided constraints on the charge-to-mass ratio at a 68% credible level, yielding a value of 0.72 [36–38]. Additionally, studies on the bremsstrahlung emission profile of BHs [39, 40] have established an observational upper bound on the charge of Sgr A*, which $\lesssim 3 \times 10^8 C$. The presence of electric charge in BHs could also alter the waveform of GW during the coalescence of binary compact objects. This modification provides a novel avenue to constrain BH charges through GW events. Specifically, the inspiral, merger-ringdown signals, and electromagnetic counterparts associated with GWs can individually provide bounds on the charge of BHs [41–46].

* Corresponding author: wanght@pku.edu.cn

† Corresponding author: jzyan@pmo.ac.cn

TABLE I. Constraints on α_{EdGB} in previous studies

LMXB	NS	GW(BBH)		GW(NSBH)		Stacking		
		0.27 (0.254) ^a	GW190814 [25]			0.25 (0.98) ^b	GWTC-3 [25]	
		5.6	GW170608 [26]	1.1 (0.87)	GW200115 [25]	1.18	GW200105, GW200115, GW190814 and BBHs [27]	
$\sqrt{\alpha_{\text{EdGB}}}$ [km]	1.9 [23]	1.29 [24]	4.3	GW151226 [28]	1.33	GW200115 [27]	1.85	GWTC-1 [29]
			0.4	GW190814 [30]	2.18	GW190814 [25]	1.7	GWTC-1 and GWTC-2 [31]
			0.8	GW190814 [32]				

Notes. Values in parentheses represent results from analyses with merge-ringdown contributions. Assuming GW190814 as a NSBH merger, the constraints are 0.98.

In this work, by incorporating modifications to the GW phase within the ppE framework, we conduct Bayesian analyses using GW230529 data to constrain parameters in EdGB theories and the potential charge of black holes. The refined results from the inspiral signal of the GW data establish more stringent limits compared to previous studies. The methodology employed, involving the ppE framework and Bayesian analysis, is detailed in Section II. The main findings are discussed in Section III, and a summary of the study is presented in Section IV. Throughout this paper, we adopt units where $G = c = 1$, unless otherwise specified.

II. METHOD

The ppE framework was originally introduced to investigate possible deviations from GR and probe alternative theories of gravity [3]. The ppE waveform model in inspiral regime is formulated as follows $\tilde{h}_{\text{ppE}}(f) = \tilde{h}_{\text{GR}}(f)(1 + \alpha u^a)e^{i\beta u^b}$, where (α, a, β, b) are the ppE parameters. Here $u = \pi M f$ is the inspiral reduced frequency, and $M = (m_1 m_2)^{3/5} / (m_1 + m_2)^{1/5}$ is the chirp mass. The work by Tahura *et al.* [28] shows that sole phase corrections are capable of providing reliable constraints. Consequently, we focus on phase corrections arising from non-Kerr effects. The ppE waveform model can be simplified as $\tilde{h}(f) = A(f)e^{i\Psi_{\text{GR}}(f) + i\beta_{\text{EdGB,charge}}(\pi M f)^b}$, where the additional modifications to the GW phase appear at -1PN for both EdGB gravity and charge effect of BHs. Specifically, for EdGB gravity, the ppE parameters are [47]

$$\beta_{\text{EdGB}} = -\frac{5}{7168} \frac{(m_1^2 s_2^{\text{EdGB}} - m_2^2 s_1^{\text{EdGB}})^2}{\eta^{18/5} M^4} \frac{16\pi\alpha_{\text{EdGB}}^2}{M^4}, \quad (1)$$

where, $\eta = m_1 m_2 / M^2$ is the symmetric mass ratio, $M = m_1 + m_2$ is the total mass, and $s_i^{\text{EdGB}} = 2(\sqrt{1 - \chi_i^2} - 1 + \chi_i^2) / \chi_i^2$ are the dimensionless BH charges in EdGB gravity. Here, $\chi_i = \vec{S}_i \cdot \hat{L} / m_i^2$ represents the dimensionless spins component of the BHs in the direction of the orbital angular momentum. In NSBH binary system, the scalar charges s_i^{EdGB} vanish for neutron stars [48]. Considering that the phase corrections stemming from EdGB modifications are small perturbations compared to the GR contributions, the coupling parameters must satisfy the small coupling approximation $\zeta_{\text{EdGB}} = 16\pi\alpha_{\text{EdGB}}^2 / m_s^4 < 1$. Following Refs. [25, 27, 31],

we use the threshold

$$\sqrt{\alpha_{\text{EdGB}}} \leq \frac{m_s}{(32\pi)^{1/4}} = 0.466 \frac{m_s}{M_\odot} [\text{km}], \quad (2)$$

where m_s is the smallest mass scale of a system and M_\odot means solar mass.

In general, the waveform models of GW do not include the charge of BHs. By considering the charge effects as a perturbation in the inspiral stage, the corrections due to the electric dipole radiation on the waveform can be captured by the ppE framework. The coefficients can be written as [35, 41, 49],

$$\begin{aligned} \Delta\Psi_{\text{charge}} &= \beta_{\text{charge}}(\pi M f)^b \\ &= -\frac{5}{3584} \eta^{2/5} \zeta^2 \kappa^2 (\pi \kappa M f)^{-7/3}, \end{aligned} \quad (3)$$

where the difference between the charge of binary stars is denoted as $\zeta = |\lambda_1 - \lambda_2| / \sqrt{1 - \lambda_1 \lambda_2}$, with $\lambda_i = q_i / m_i$ representing the charge-to-mass ratio and q_i representing the electric charge. The above equation is applicable to binary systems where one or both components possess an electric charge. Although neutron stars are typically regarded as electrically neutral, several theoretical models propose the existence of charged neutron stars [50–52]. Consequently, we focus on deriving constraints on the combination of electric charges of the binary components, rather than setting λ_{NS} to zero. In this work, the effects of charge are considered as small perturbations, i.e., $\kappa = 1 - \lambda_1 \lambda_2 \approx 1$.

In the context of data processing, the posterior probability distribution of parameters ϑ given data d is defined by the following expression:

$$p(\vartheta|d, \mathcal{H}) = \frac{p(d|\vartheta, \mathcal{H})p(\vartheta|\mathcal{H})}{p(d|\mathcal{H})} = \frac{p(d|\vartheta, \mathcal{H})p(\vartheta|\mathcal{H})}{\int d\vartheta p(d|\vartheta, \mathcal{H})p(\vartheta|\mathcal{H})}, \quad (4)$$

as derived from Bayes's theorem. Here, $p(d|\vartheta, \mathcal{H})$, $p(\vartheta|\mathcal{H})$ and $p(d|\mathcal{H})$ represent the likelihood, the prior, and the evidence, respectively. In cases of stationary and Gaussian noise, the likelihood is modeled as:

$$p(d|\vartheta, \mathcal{H}) \propto \exp\left[-\frac{1}{2} \sum_{j=1}^N (d_j - h_j|\vartheta)(d_j - h_j|\vartheta)\right], \quad (5)$$

where d_j and $h_j(\vartheta)$ denote the data and the waveform model for the i -th detector, respectively. The noise-weighted inner product $(a(t)|b(t))$ is defined by:

$$(a(t)|b(t)) = 2\mathcal{R} \int_{f_{\text{low}}}^{f_{\text{high}}} \frac{\tilde{a}^*(f)\tilde{b}(f) + \tilde{a}(f)\tilde{b}^*(f)}{S_n(f)} df, \quad (6)$$

where f_{low} and f_{high} are the high-pass and low-pass cutoff frequencies of GW data, * indicates the complex conjugate, and $S_n(f)$ is the power spectral density. In this study, we primarily examine the inspiral phase. According to Refs. [53, 54], the transition frequency from inspiral to intermediate phase is given by the relation $Mf_t = 0.018$, where M is the detector frame's total mass of the binary. Therefore, we set the high-pass and low-pass cutoff frequencies at $f_{\text{low}} = 20$ Hz and $f_{\text{high}} = 0.018/[(m_1 + m_2)] = 584$ Hz, respectively. We conduct Bayesian parameter estimation for GW230529 using the BILBY package [55] and the DYNESTY sampler [56] with 1000 live points. The number of sampling steps ranges from a minimum of 100 to a maximum of 5000. When bounding electric charges of the binary, we set $\kappa = 1$ and sample over ζ . Uniform priors are assigned for $\sqrt{\alpha_{\text{EdGB}}}$ and ζ over the intervals $[0, 5]$ km and $[0, \sqrt{2}]$, respectively. For other parameters, we adhere to the priors utilized in Ref. [1].

III. RESULTS

To date, solar mass black holes have not been observed yet. GW230529 is more plausibly a NSBH merger [57, 58], although the possibility of a binary black hole (BBH) merger cannot be entirely ruled out based on sole GW data [59]. This study, therefore, investigates the constraints imposed by GW230529 on the interpretation of NSBH mergers. We present the posterior distributions derived from Bayesian analyses using various waveform models in Figure 1 and 2. The Figure 1 displays results that include -1PN corrections, while the Figure 2 incorporates results with higher-order PN corrections. We obtain the constraints under various waveform models, including IMRPhenomNSBH [60] and IMRPhenomPv2_NRTidalv2 [61]. Given the large mass ratio of GW230529, the tidal effects of the secondary star on the waveform are minimal. Accordingly, it is feasible to use the IMRPhenomXPHM model [62], initially developed for BBH mergers, to analyze NSBH events. For IMRPhenomPv2_NRTidalv2 and IMRPhenomNSBH waveforms, uncertainties related to the equation of state (EoS) of neutron stars are not considered. Specifically, the primary star's tidal deformability is assumed to be $\Lambda_1 = 0$, whereas the secondary star's tidal deformability, Λ_2 , is determined using the BSK24 EoS [63–65], consistent with the approach in Ref. [1].

The constraints established by GW230529 on α_{EdGB} are $\lesssim 0.415$ km for IMRPhenomPv2_NRTidalv2, $\lesssim 0.361$ km for IMRPhenomNSBH, and $\lesssim 0.298$ km for IMRPhenomXPHM with tidal effects of the event neglected. Notably, IMRPhenomXPHM provides marginally better constraints on $\sqrt{\alpha_{\text{EdGB}}}$ compared to other two waveform models, likely due to its more precise modeling. For EdGB gravity, the leading corrections dominate at frequencies $f \lesssim 200$ Hz, whereas higher order corrections become significant at higher frequencies. Given the relatively low mass of the components in GW230529, the inspiral signals extend to higher frequencies, necessitating further investigation into α_{EdGB} constraints in conjunction with advanced post-Newtonian (PN) phase corrections. The ppE framework, incorporating phase corrections

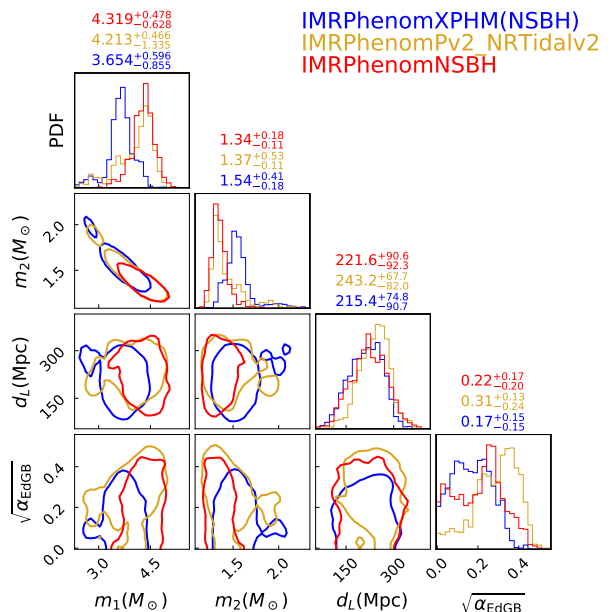


FIG. 1. Posterior probability distributions of some key parameters, e.g., the gravitational coupling constant $\sqrt{\alpha_{\text{EdGB}}}$, the masses of the primary (m_1) and secondary (m_2) components in the detector frame, and the luminosity distance (d_L) for GW230529. The golden, red, and blue colors represent analyses conducted with the IMRPhenomPv2_NRTidalv2, IMRPhenomNSBH, and IMRPhenomXPHM (tidal effects are omitted) waveform models, respectively. The contours indicate the 90% credible intervals. The diagonal entries display the median values and the corresponding 90% interval ranges.

up to 2PN order, is expressed as $\delta\Psi = \sum_i \beta_i^{\text{PPE}} v^{-5+2i}$, where $v = (\pi M f)^{1/3}$ and i represents PN orders of $-1, 0, 0.5, 1, 1.5$, and 2. The coefficients β_i are detailed in Ref. [27]. Incorporating higher-order corrections of EdGB gravity, the 90% upper bounds are 0.260 km using the IMRPhenomXPHM model and 0.358 km using the IMRPhenomPv2_NRTidalv2 model, representing improvements of 13% and 14%, respectively. As illustrated in Figure 2, the median value and upper limit of $\sqrt{\alpha_{\text{EdGB}}}$ have shown enhancements across all waveform models. We also check the validity of the small coupling approximation. As shown in Figure 3, we find that GW230529 can place meaningful constraints on $\sqrt{\alpha_{\text{EdGB}}}$ for all results. It is crucial to note that the higher PN corrections applied here do not account for tidal effects, which is outside the scope of this study. A summary of these bounds is provided in Table II.

TABLE II. The 90% upper bounds on $\sqrt{\alpha_{\text{EdGB}}}$ from GW230529

Waveform models	NSBH	NSBH (HPN)	Improvement
IMRPhenomXPHM	0.298	0.260	13%
IMRPhenomPv2_NRTidalv2	0.415	0.358	14%
IMRPhenomNSBH	0.361	0.350	3%

When investigating the potential charge of the binary, we do not consider non-GR gravity effects. Analysis conducted with the IMRPhenomPv2_NRTidalv2 and IMRPhenomNSBH

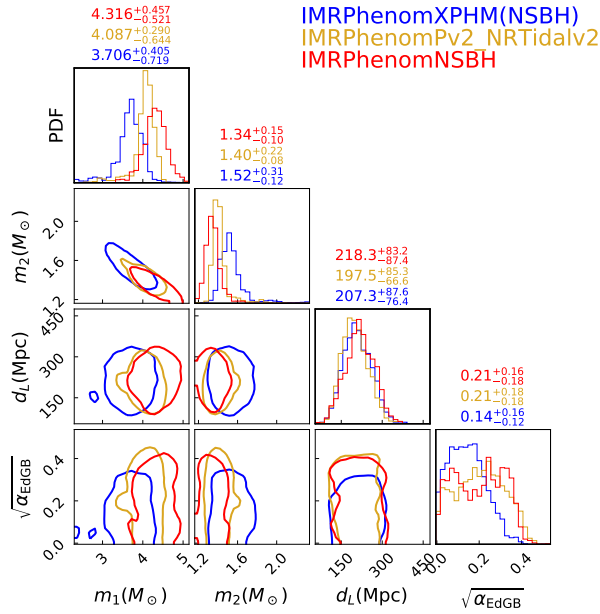


FIG. 2. Similar to Figure 1 but for results with inclusion of high order corrections.

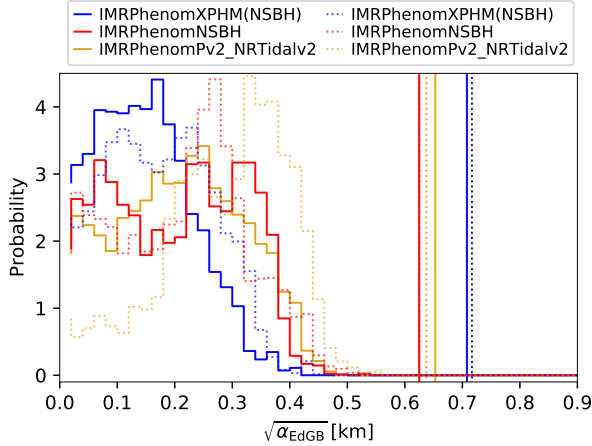


FIG. 3. Comparison between the posterior distributions of $\sqrt{\alpha_{\text{EdGB}}}$ and the requirements of the small coupling approximation. The vertical lines represent the thresholds of $\sqrt{\alpha_{\text{EdGB}}}$ given by Eq. (2). It should be noted that the majority of the posterior distributions from each parameter estimation analysis fall within the threshold of the small coupling approximation. The solid and dotted lines denote results obtained with high order corrections and -1PN corrections, respectively.

waveform models constrains the parameter ζ to be less than 0.024 and 0.027 at the 90% credible upper level, respectively. When neglecting the tidal effects and utilizing the IMRPhenomXPHM waveform model, the constraint on the charge tightens to $\zeta \leq 0.019$. Figure 4 illustrates the posterior distribution of ζ for GW230529. These constraints are more stringent than the previously most restrictive limit of 0.21 at the 90% credible level, established by GW170608 [41]. The tight-

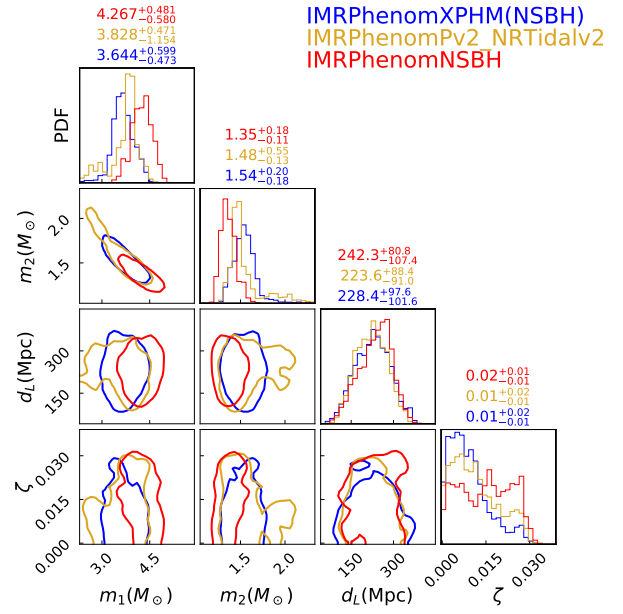


FIG. 4. Posterior probability distributions of some key parameters, e.g., the combination of charges ζ , the masses of the primary (m_1) and secondary (m_2) components in the detector frame, and the luminosity distance (d_L) for GW230529. The golden, red, and blue colors represent analyses conducted with the IMRPhenomPv2_NRTidalv2, IMRPhenomNSBH, and IMRPhenomXPHM (tidal effects are omitted) waveform models, respectively. The contours indicate the 90% credible intervals. The diagonal entries display the median values and the corresponding 90% interval ranges.

est bound on the charge-to-mass ratio of a single BH is 0.3, achieved at 90% credibility by the remnant BH of GW150914 [42]. The constraints on the charge-to-mass ratio can be improved to 0.2 with merger-ringdown signals of a GW150914-like event for the Einstein Telescope [46]. Considering potential electromagnetic counterparts associated with GW200105, the estimated upper limit on the charge-to-mass ratio for the BH is 4.3×10^{-3} [45]. Due to the unknown charge of NS in GW230529, the posterior distributions of the charge-to-mass ratio cannot be obtained from the distributions of ζ . Nevertheless, even when the charge-to-mass ratio of an NS reaches as high as 0.1¹, the distribution of κ (converted from the posterior of ζ) is consistent with the small perturbation assumption ($\kappa \approx 1$) used in the parameter estimation. Consequently, the constraints on ζ provide meaningful limits.

IV. CONCLUSIONS

In this work, we reanalyzed the GW event GW230529 within the ppE framework to impose constraints on the cou-

¹ The charge of a uniformly magnetized NS is $Q = \frac{2}{3}\Omega B_p R_{\text{NS}}^3/c$ [45, 66]. For a $1.4M_\odot$ NS with $B_p = 10^{16}$ G, $P = 1$ ms and $R_{\text{NS}} = 12$ km, the charge-to-mass ratio is 3.36×10^{-3} .

pling parameters of EdGB gravity and the charge of this binary system. Given that GW230529 is a NSBH merger, we established an upper bound of $\sqrt{\alpha_{\text{EdGB}}} \lesssim 0.298$ km at the 90% credible level, with different waveform models resulting in slight variations in the constraints. By incorporating higher-order post-Newtonian phase corrections, we achieved tighter bounds, with $\sqrt{\alpha_{\text{EdGB}}} \lesssim 0.260$ km. These are the first constraints derived from low mass NSBH mergers with higher-order post-Newtonian corrections. Considering the unknown nature of GW190814, the bounds presented here are the most stringent bounds among all robust results. The degree of improvement in these constraints varies across different waveform models. In addition to its implications for EdGB gravity, GW230529 also establishes a stringent limit on the charge of coalescing binary systems of compact objects, with an upper limit of 0.024 at the 90% credible level. This is the first constraint from a NSBH system with GW data. While these con-

straints are less stringent than those derived from X-ray data, which estimate the charge-to-mass ratio of BHs to be on the order of $\lambda \sim 10^{-18}$, they nonetheless provide valuable insights obtained from GW observations.

ACKNOWLEDGMENTS

The authors thank Yin-Jie Li, Ran Chen, and Wen-qing Guo for useful discussion. This work is supported in part by the National Natural Science Foundation of China under grant Nos. U2031205, 11733009, 12233011, 12303056, and 12247152, the China Postdoctoral Science Foundation (2022TQ0011), the Project for Special Research Assistant of the Chinese Academy of Sciences, and by the General Fund (No. 2023M733736) of the China Postdoctoral Science Foundation.

-
- [1] The LIGO Scientific Collaboration, the Virgo Collaboration, and the KAGRA Collaboration, “Observation of Gravitational Waves from the Coalescence of a $2.5 - 4.5 M_{\odot}$ Compact Object and a Neutron Star,” *arXiv e-prints*, [arXiv:2404.04248 \(2024\)](#).
- [2] Y.-Z. Fan, M.-Z. Han, J.-L. Jiang, D.-S. Shao, and S.-P. Tang, “Maximum gravitational mass $M_{\text{TOV}} = 2.25^{+0.08}_{-0.07} M_{\odot}$ inferred at about 3% precision with multimessenger data of neutron stars,” *Phys. Rev. D* **109**, 043052 (2024).
- [3] N. Yunes and F. Pretorius, “Fundamental theoretical bias in gravitational wave astrophysics and the parametrized post-Einsteinian framework,” *Phys. Rev. D* **80**, 122003 (2009).
- [4] N. Yunes, K. Yagi, and F. Pretorius, “Theoretical physics implications of the binary black-hole mergers GW150914 and GW151226,” *Phys. Rev. D* **94**, 084002 (2016).
- [5] S. Nojiri and S. D. Odintsov, “Unified cosmic history in modified gravity: from F(R) theory to Lorentz non-invariant models,” *Phys. Rept.* **505**, 59–144 (2011).
- [6] S. Nojiri, S. D. Odintsov, and V. K. Oikonomou, “Modified Gravity Theories on a Nutshell: Inflation, Bounce and Late-time Evolution,” *Phys. Rept.* **692**, 1–104 (2017).
- [7] H. O. Silva, J. Sakstein, L. Gualtieri, T. P. Sotiriou, and E. Berti, “Spontaneous Scalarization of Black Holes and Compact Stars from a Gauss-Bonnet Coupling,” *Phys. Rev. Lett.* **120**, 131104 (2018).
- [8] P. G. S. Fernandes, P. Carrilho, T. Clifton, and D. J. Mulryne, “The 4D Einstein–Gauss–Bonnet theory of gravity: a review,” *Class. Quant. Grav.* **39**, 063001 (2022).
- [9] P. G. S. Fernandes, D. J. Mulryne, and J. F. M. Delgado, “Exploring the small mass limit of stationary black holes in theories with Gauss-Bonnet terms,” *Classical and Quantum Gravity* **39**, 235015 (2022).
- [10] M. Elley, H. O. Silva, H. Witek, and N. Yunes, “Spin-induced dynamical scalarization, descalarization, and stealthness in scalar-Gauss-Bonnet gravity during a black hole coalescence,” *Phys. Rev. D* **106**, 044018 (2022).
- [11] S. Nojiri and S. D. Odintsov, “Propagation speed of gravitational wave in scalar–Einstein–Gauss-Bonnet gravity,” *Nucl. Phys. B* **998**, 116423 (2024).
- [12] S. Nojiri, S. D. Odintsov, and V. K. Oikonomou, “Propagation of gravitational waves in Einstein-Gauss-Bonnet gravity for cosmological and spherically symmetric spacetimes,” *Phys. Rev. D* **109**, 044046 (2024).
- [13] K. Chakravarti, R. Ghosh, and S. Sarkar, “Constraining the topological Gauss-Bonnet coupling from GW150914,” *Phys. Rev. D* **106**, L041503 (2022).
- [14] P. Kanti, N. E. Mavromatos, J. Rizos, K. Tamvakis, and E. Winstanley, “Dilatonic black holes in higher curvature string gravity,” *Phys. Rev. D* **54**, 5049–5058 (1996).
- [15] T. Torii, H. Yajima, and K.-I. Maeda, “Dilatonic black holes with a Gauss-Bonnet term,” *Phys. Rev. D* **55**, 739–753 (1997).
- [16] J. Tan, J.-d. Zhang, H.-M. Fan, and J. Mei, “Constraining the EdGB Theory with Extreme Mass-Ratio Inspirals,” *arXiv e-prints*, [arXiv:2402.05752 \(2024\)](#).
- [17] C. Shi, M. Ji, J.-d. Zhang, and J. Mei, “Testing general relativity with TianQin: The prospect of using the inspiral signals of black hole binaries,” *Phys. Rev. D* **108**, 024030 (2023).
- [18] C.-Y. Shao, Y. Hu, and C.-G. Shao, “Parameter estimation for Einstein-dilaton-Gauss-Bonnet gravity with ringdown signals,” *Chinese Physics C* **47**, 105101 (2023).
- [19] W. Luo, C. Liu, and Z.-K. Guo, “Constraints on Einstein-dilaton Gauss-Bonnet gravity with Taiji,” *Eur. Phys. J. C* **84**, 394 (2024).
- [20] Z. Carson and K. Yagi, “Probing Einstein-dilaton Gauss-Bonnet Gravity with the inspiral and ringdown of gravitational waves,” *Phys. Rev. D* **101**, 104030 (2020).
- [21] M. Rahman, S. Kumar, and A. Bhattacharyya, “Gravitational wave from extreme mass-ratio inspirals as a probe of extra dimensions,” *JCAP* **01**, 046 (2023).
- [22] A. Chowdhuri, A. Bhattacharyya, and S. Kumar, “Prospects of detecting deviations to Kerr geometry with radiation reaction effects in EMRIs,” *JCAP* **04**, 001 (2024).
- [23] K. Yagi, “New constraint on scalar gauss-bonnet gravity and a possible explanation for the excess of the orbital decay rate in a low-mass x-ray binary,” *Phys. Rev. D* **86**, 081504 (2012).
- [24] A. Saffer and K. Yagi, “Tidal deformabilities of neutron stars in scalar-Gauss-Bonnet gravity and their applications to multimessenger tests of gravity,” *Phys. Rev. D* **104**, 124052 (2021).
- [25] B. Wang, C. Shi, J.-d. Zhang, Y.-M. Hu, and J. Mei, “Constraining the Einstein-dilaton-Gauss-Bonnet theory with higher harmonics and the merger-ringdown contribution using GWTC-3,” *Phys. Rev. D* **108**, 044061 (2023).

- [26] R. Nair, S. Perkins, H. O. Silva, and N. Yunes, “Fundamental Physics Implications for Higher-Curvature Theories from Binary Black Hole Signals in the LIGO-Virgo Catalog GWTC-1,” *Phys. Rev. Lett.* **123**, 191101 (2019).
- [27] Z. Lyu, N. Jiang, and K. Yagi, “Constraints on Einstein-dilation-Gauss-Bonnet gravity from black hole-neutron star gravitational wave events,” *Phys. Rev. D* **105**, 064001 (2022).
- [28] S. Tahura, K. Yagi, and Z. Carson, “Testing gravity with gravitational waves from binary black hole mergers: Contributions from amplitude corrections,” *Phys. Rev. D* **100**, 104001 (2019).
- [29] K. Yamada, T. Narikawa, and T. Tanaka, “Testing massive-field modifications of gravity via gravitational waves,” *Progress of Theoretical and Experimental Physics* **2019**, 103E01 (2019).
- [30] H.-T. Wang, S.-P. Tang, P.-C. Li, M.-Z. Han, and Y.-Z. Fan, “Tight constraints on Einstein-dilation-Gauss-Bonnet gravity from GW190412 and GW190814,” *Phys. Rev. D* **104**, 024015 (2021).
- [31] S. E. Perkins, R. Nair, H. O. Silva, and N. Yunes, “Improved gravitational-wave constraints on higher-order curvature theories of gravity,” *Phys. Rev. D* **104**, 024060 (2021).
- [32] G. Carullo, “Enhancing modified gravity detection from gravitational-wave observations using the parametrized ring-down spin expansion coefficients formalism,” *Phys. Rev. D* **103**, 124043 (2021).
- [33] L. Liu, Z.-K. Guo, R.-G. Cai, and S. P. Kim, “Merger rate distribution of primordial black hole binaries with electric charges,” *Phys. Rev. D* **102**, 043508 (2020).
- [34] R. Maier and M. C. e Silva, “Charged black holes from interacting vacuum,” (2024), [arXiv:2405.10293 \[gr-qc\]](https://arxiv.org/abs/2405.10293).
- [35] V. Cardoso, C. F. B. Macedo, P. Pani, and V. Ferrari, “Black holes and gravitational waves in models of minicharged dark matter,” *JCAP* **05**, 054 (2016), [Erratum: *JCAP* **04**, E01 (2020)].
- [36] P. Kocherlakota *et al.* (Event Horizon Telescope), “Constraints on black-hole charges with the 2017 EHT observations of M87*,” *Phys. Rev. D* **103**, 104047 (2021).
- [37] K. Akiyama *et al.* (Event Horizon Telescope), “First Sagittarius A* Event Horizon Telescope Results. VI. Testing the Black Hole Metric,” *Astrophys. J. Lett.* **930**, L17 (2022).
- [38] S. G. Ghosh and M. Afrin, “An Upper Limit on the Charge of the Black Hole Sgr A* from EHT Observations,” *Astrophys. J.* **944**, 174 (2023).
- [39] M. Karouzos, “Charge in the hole,” *Nature Astronomy* **2**, 764–764 (2018).
- [40] M. Zajaček, A. Tursunov, A. Eckart, and S. Britzen, “On the charge of the Galactic centre black hole,” *Mon. Not. Roy. Astron. Soc.* **480**, 4408–4423 (2018).
- [41] H.-T. Wang, P.-C. Li, J.-L. Jiang, G.-W. Yuan, Y.-M. Hu, and Y.-Z. Fan, “Constraints on the electric charges of the binary black holes with GWTC-1 events,” *Eur. Phys. J. C* **81**, 769 (2021).
- [42] G. Bozzola and V. Paschalidis, “General Relativistic Simulations of the Quasicircular Inspiral and Merger of Charged Black Holes: GW150914 and Fundamental Physics Implications,” *Phys. Rev. Lett.* **126**, 041103 (2021).
- [43] H.-T. Wang, S.-P. Tang, P.-C. Li, and Y.-Z. Fan, “Quasinormal modes of the Kerr-Newman black hole: GW150914 and fundamental physics implications,” *Phys. Rev. D* **104**, 104063 (2021).
- [44] G. Carullo, D. Laghi, N. K. Johnson-McDaniel, W. Del Pozzo, Ó. J. C. Dias, M. Godazgar, and J. E. Santos, “Constraints on Kerr-Newman black holes from merger-ringdown gravitational-wave observations,” *Phys. Rev. D* **105**, 062009 (2022).
- [45] H.-Y. Yuan, H.-J. Lü, J. Rice, and E.-W. Liang, “Constraining the charge of a black hole with electromagnetic radiation from a black hole-neutron star system,” *Phys. Rev. D* **108**, 083018 (2023).
- [46] H.-P. Gu, H.-T. Wang, and L. Shao, “Constraints on charged black holes from merger-ringdown signals in GWTC-3 and prospects for the Einstein Telescope,” *Phys. Rev. D* **109**, 024058 (2024).
- [47] K. Yagi, L. C. Stein, N. Yunes, and T. Tanaka, “Post-Newtonian, quasicircular binary inspirals in quadratic modified gravity,” *Phys. Rev. D* **85**, 064022 (2012).
- [48] K. Yagi, L. C. Stein, and N. Yunes, “Challenging the presence of scalar charge and dipolar radiation in binary pulsars,” *Phys. Rev. D* **93**, 024010 (2016).
- [49] O. Christiansen, J. Beltrán Jiménez, and D. F. Mota, “Charged Black Hole Mergers: Orbit Circularisation and Chirp Mass Bias,” *Class. Quant. Grav.* **38**, 075017 (2021).
- [50] M. A. Ruderman and P. G. Sutherland, “Theory of pulsars: polar gaps, sparks, and coherent microwave radiation,” *Astrophys. J.* **196**, 51–72 (1975).
- [51] C. R. Ghezzi, “Relativistic structure, stability, and gravitational collapse of charged neutron stars,” *Phys. Rev. D* **72**, 104017 (2005).
- [52] M. Fabbrichesi and A. Urbano, “Charged neutron stars and observational tests of a dark force weaker than gravity,” *JCAP* **06**, 007 (2020).
- [53] S. Khan, S. Husa, M. Hannam, F. Ohme, M. Pürrer, X. J. Forteza, and A. Bohé, “Frequency-domain gravitational waves from nonprecessing black-hole binaries. II. A phenomenological model for the advanced detector era,” *Phys. Rev. D* **93**, 044007 (2016).
- [54] B. P. Abbott, R. Abbott, T. D. Abbott, and et al. (The LIGO Scientific Collaboration and the Virgo Collaboration), “Tests of general relativity with the binary black hole signals from the ligo-virgo catalog gwtc-1,” *Phys. Rev. D* **100**, 104036 (2019).
- [55] G. Ashton *et al.*, “BILBY: A user-friendly Bayesian inference library for gravitational-wave astronomy,” *Astrophys. J. Suppl.* **241**, 27 (2019).
- [56] J. S. Speagle, “dynesty: a dynamic nested sampling package for estimating Bayesian posteriors and evidences,” *Mon. Not. Roy. Astron. Soc.* **493**, 3132–3158 (2020).
- [57] J.-P. Zhu, R.-C. Hu, Y. Kang, B. Zhang, H. Tong, L. Shao, and Y. Qin, “Formation of GW230529 from Isolated Binary Evolution and Its Electromagnetic Counterparts,” [arXiv e-prints](https://arxiv.org/abs/2404.10596), [arXiv:2404.10596](https://arxiv.org/abs/2404.10596) (2024).
- [58] K. Chandra, I. Gupta, R. Gamba, R. Kashyap, D. Chattopadhyay, A. Gonzalez, S. Bernuzzi, and B. S. Sathyaprakash, “Everything everywhere all at once: A detailed study of GW230529,” [arXiv e-prints](https://arxiv.org/abs/2405.03841), [arXiv:2405.03841](https://arxiv.org/abs/2405.03841) (2024).
- [59] Q.-G. Huang, C. Yuan, Z.-C. Chen, and L. Liu, “GW230529_181500: A Potential Primordial Binary Black Hole Merger in the Mass Gap,” [arXiv e-prints](https://arxiv.org/abs/2404.05691), [arXiv:2404.05691](https://arxiv.org/abs/2404.05691) (2024).
- [60] J. E. Thompson, E. Fauchon-Jones, S. Khan, E. Nitoglia, F. Pannarale, T. Dietrich, and M. Hannam, “Modeling the gravitational wave signature of neutron star black hole coalescences,” *Phys. Rev. D* **101**, 124059 (2020).
- [61] T. Dietrich, A. Samajdar, S. Khan, N. K. Johnson-McDaniel, R. Dudi, and W. Tichy, “Improving the NRTidal model for binary neutron star systems,” *Phys. Rev. D* **100**, 044003 (2019).
- [62] G. Pratten, C. García-Quirós, M. Colleoni, A. Ramos-Buades, H. Estellés, M. Mateu-Lucena, R. Jaume, M. Haney, D. Keitel, J. E. Thompson, and S. Husa, “Computationally efficient models for the dominant and subdominant harmonic modes of precessing binary black holes,” *Phys. Rev. D* **103**, 104056 (2021).
- [63] S. Goriely, N. Chamel, and J. M. Pearson, “Hartree-fock-bogoliubov nuclear mass model with 0.50 mev accuracy based

- on standard forms of skyrme and pairing functionals,” *Phys. Rev. C* **88**, 061302 (2013).
- [64] J. M. Pearson, N. Chamel, A. Y. Potekhin, A. F. Fantina, C. Ducoin, A. K. Dutta, and S. Goriely, “Unified equations of state for cold non-accreting neutron stars with Brussels–Montreal functionals – I. Role of symmetry energy,” *Mon. Not. Roy. Astron. Soc.* **481**, 2994–3026 (2018), [Erratum: *Mon. Not. Roy. Astron. Soc.* 486, 768 (2019)].
- [65] L. Perot, N. Chamel, and A. Sourie, “Role of the symmetry energy and the neutron-matter stiffness on the tidal deformability of a neutron star with unified equations of state,” *Phys. Rev. C* **100**, 035801 (2019).
- [66] M. A. Ruderman and P. G. Sutherland, “Theory of pulsars: Polar caps, sparks, and coherent microwave radiation,” *Astrophys. J.* **196**, 51 (1975).